CSGB CENTRE FOR STOCHASTIC GEOMETRY AND ADVANCED BIOIMAGING

Vinay Suryaprakash, Jesper Møller and Gerhard P. Fettweis

On the Modeling and Analysis of Heterogeneous Radio Access Networks using a Poisson Cluster Process

No. 03, February 2014

On the Modeling and Analysis of Heterogeneous Radio Access Networks using a Poisson Cluster Process

Vinay Suryaprakash*, Jesper Møller**, and Gerhard P. Fettweis*
*Vodafone Chair Mobile Communications Systems, TU Dresden, Germany
(vinay.suryaprakash,gerhard.fettweis)@ifn.et.tu-dresden.de
**Department of Mathematical Sciences, Aalborg University, Fredrik Bajers Vej 7G, DK-9220, Aalborg. e-mail: jm@math.aau.dk

Abstract

Future mobile networks are visualized as networks that consist of more than one type of base station to cope with rising user demands. Such networks are referred to as heterogeneous networks. There have been various attempts at modeling and optimization of such networks using spatial point processes, some of which are alluded to (later) in this paper. We model a heterogeneous network consisting of two types of base stations by using a particular Poisson cluster process model. The main contributions are two-fold. First, a complete description of the interference in heterogeneous networks is derived in the form of its Laplace functional. Second, using an asymptotic convergence result which was shown in our previous work, we derive the expressions for the mean and variance of the distribution to which the interference converges. The utility of this framework is discussed for both the contributions.

Index Terms

Heterogeneous wireless networks, Poisson cluster process, interference, probability of coverage.

I. Introduction

HETEROGENEOUS networks (HetNets) are widely regarded, by industry and academia alike, as the solution to the problem of being able to cope with an ever increasing demand for ubiquitous coverage along with high data rates. HetNets, in general, involve deploying different types of smaller base stations in a given area if a macro base station is unable to deal with user demands at a given location. This method of deployment results in fairly intricate and random deployment topologies. Till recently, most efforts undertaken to analyze and improve HetNets have been through extensive simulations. Preliminary efforts involved carrying out simulations using a hexagonal grid of macro base stations with micro base stations that are randomly distributed within the cell areas of the macro base station. This model is far from realistic when it comes to mimicking a real world deployment, since geographical and man-made features (such as mountains, lakes, rivers, monuments, streets, etc.) rarely allow base station deployments that mimic a hexagonal grid. Another limitation of this approach is that most simulations are run on proprietary simulators, and it is extremely difficult to verify and compare these results. These limitations have resulted in recent efforts to model such networks analytically. Theoretic methods enable us to analyze these networks while saving significant amounts of time and effort required in carrying out simulations. These methods also provide a bench mark against which results from different proprietary simulators can be compared.

Unfortunately, a comprehensive mathematical analysis of such scenarios also turns out to be a very arduous task. However, a theoretic analysis of these networks at a system level is much simpler. Therefore, simplified system models have been used to understand relationships between various performance metrics, such as probability of coverage or spectral efficiency, and the effectiveness of wireless networks. One

such method of theoretic analysis is the use of stochastic geometry or spatial point process theory. For homogeneous networks, there are several well known works by Baccelli et al., such as [1], [2] and [3], which use Poisson processes, and more recently, works like [7] and [15] have tried to use models based on Ginibre point processes. In this case, the main difference is that Ginibre point process models are slightly more repulsive or regular than Poisson point processes, i.e., the tendency for clustering in the former case is less pronounced.

A recent paper by Dhillon et al., [4], models HetNets as networks which are essentially superpositions of $k-1$ layers of independent Poisson processes, where each layer represents a different type of base station. Their paper happens to be one of the first attempts at trying to model and analyze HetNets theoretically. Though its findings are very insightful, as the layers are independent, the deployment of a smaller (essentially supplementary) base station is independent of the ability of the larger base station to cater to the demands in the area. This, however, is not completely accurate for most dense urban deployments where HetNets are most desired. In most cases, smaller base stations are deployed within the macro cell areas wherever, and whenever the need arises. Hence, the smaller base stations are (in some sense) clustered[1] around the macro base station. This kind of clustering can be modeled by a Poisson cluster process as specified in this paper.

A. Contributions and organization of the paper

A topic of crucial importance, and hence, common to all of the above approaches (whether simulation based or theoretic) is understanding, and describing the behavior of the interference in the area. A similar approach is followed in this paper. Our primary contribution is a method to analyze interference in HetNets using a Poisson cluster process which allows computation of certain performance metrics (probability of coverage, etc.) based on which further network optimization can take place. The contribution can be divided into two parts. First, we begin by deriving a general expression for the interference based on system parameters such as transmit power, pathloss, fading, etc. An application of the finding is illustrated and the insights it provides are analyzed. Second, we describe a method to estimate the interference in an area based solely on the fact that the user and base station intensities are known, and that a user is located at a particular distance from the base station closest to it. The latter method is based on a result in [14] which establishes the asymptotic convergence (in distribution) of the estimator of the interference to a Gaussian random variable. The mean and variance of the estimator of the interference are derived in this work. The utility of this method is also discussed.

The remainder of this paper is organized as follows. The introductory paragraphs of Section II describe the downlink system model. Then, Section II-A details the various notations and definitions used in this work. Section III contains the first main result which concerns the interference in HetNets, followed by Section III-A which deals with its utility. A brief recap of the asymptotic behavior of the estimator of the interference from [14] is given in Section IV, and Section IV-A contains the derivations of the mean and variance of the estimator, which form the second main result. The validity of the asymptotic behavior is verified using simulations in Section IV-B. The utility of these findings are discussed in Section IV-C. Section V contains concluding remarks, and the mathematical details along with proofs are deferred to Appendices A–C.

II. Downlink System Model

This work models base stations as points of a stationary Poisson cluster process $\Phi \subset \mathbb{R}^2$ consisting of two parts: cluster centers and cluster members, modeling the locations of macro base stations and micro base stations, respectively. Specifically, we model: i) macro base stations (the cluster centers) with

[1]Note that controlling the degree of clustering can help model scenarios where micro base station deployments are at macro base station cell edges. An illustration of this is provided in Section II.

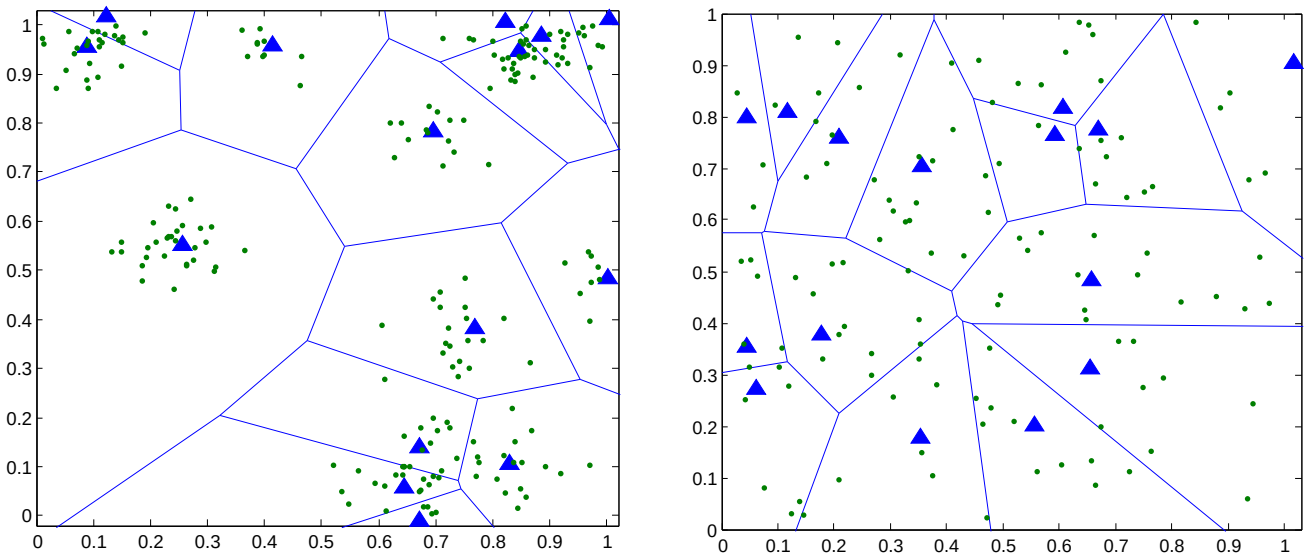

(a) Cluster members generated using a zero-mean radially symmetric Gaussian density f with variance 0.05.

(b) Cluster members generated using a zero-mean radially symmetric Gaussian density f with variance 0.5.

Fig. 1. Poisson cluster process (tessellated around parent points) with $\lambda_c = 15$ and $\lambda_m = 20$. In order to account for boundary effects, the points were generated in a larger area of 5×5 units. Note: Clustering, as illustrated by (a) and (b), becomes less pronounced as the variance of f increases. Since the clusters (as specified in Section II-A) can overlap, it can be difficult to detect the individual clusters by the naked eye.

single omni-directional antennas[2] by a stationary Poisson process $\Phi_c \subset \mathbb{R}^2$ with intensity $\lambda_c > 0$, and ii) conditioned on Φ_c, the micro base stations (the cluster members) by an inhomogeneous Poisson process $\Phi_m \subset \mathbb{R}^2$ with intensity function

$$\rho(y) = \lambda_m \sum_{x \in \Phi_c} f(y - x), \quad y \in \mathbb{R}^2, \tag{1}$$

where $\lambda_m > 0$ is a parameter and f is a continuous density function. The model can be visualized as in Figure 1, where the blue triangles represent the macro base stations and the green dots represent the micro base stations. Note that f describes how a micro base station (a cluster member) is distributed around a macro base station (its cluster center), and λ_m is the expected number of micro base stations around each macro base station. Thus, the cluster intensity and the normalized kernel "bandwidth"[3] are equal and fixed. Readers familiar with point process modeling will recognize Φ_m as a shot noise Cox process (see [9]), which as described in Section II-A, can be viewed as a Neyman-Scott cluster process (see [12]). Also note that Φ_m (not conditioned on Φ_c) is stationary with intensity $\lambda_c \lambda_m$, and the base stations, i.e. the superposition $\Phi = \Phi_c \cup \Phi_m$, form a stationary Poisson cluster process with intensity $\lambda = \lambda_c(1 + \lambda_m)$.

For the point process $\Phi = \{x_i\}$, the Voronoi cell[4] (as defined in other works such as [1], [2], [3], etc.) associated with x_i determines the area covered by a base station at x_i and is given by

$$\begin{aligned} \mathcal{C}_{x_i,\Phi} &= \left\{ z \in \mathbb{R}^2 : \text{SINR}_z \geq T' \right\} \\ &= \left\{ z \in \mathbb{R}^2 : L\left(z, x_i\right) \geq T' \left(I_{\Phi \setminus \{x_i\}}\left(z\right) + W \right) \right\}, \end{aligned}$$

[2]It is possible to include sectorization, and this will be considered in future work depending on its analytic tractability. However, sectorization has not been included because sectorization in modern networks, which typically use distributed Multiple-Input Multiple-Output (MIMO) over neighboring (overlapping) sectors as well as Cooperative Multi-Point (CoMP), leads to each site looking more like one that has an omni-directional antenna as shown in [13], and hence, sectorization becomes less important.

[3]Note:"bandwidth" is a term from mathematical literature (see e.g. [10] and references therein) which defines the spread of the cluster points around the parent point and shouldn't be confused with the definition of bandwidth in communications engineering.

[4]It is important to note that Fig.1 shows a deployment model which defines macro base station coverage areas based on a usual Voronoi tessellation (see e.g. [8]) where the cell definition is dissimilar to equation (2). The Voronoi tessellation illustrates base station deployment without any coverage holes.

where T' is a threshold and SINR_z is the Signal-to-Interference-plus-Noise Ratio at point z. Further, $L(z, x_i)$ is power received at point z from a base station at location x_i, W is the noise power, and $I_{\Phi\setminus\{x_i\}}(z)$ is the interference at point z. This can also be re-written as

$$\mathcal{C}_{x_i,\Phi} = \left\{z \in \mathbb{R}^2 : L(z, x_i) \geq T\left(I_\Phi(z) + W\right)\right\}, \tag{2}$$

where $T = T'/(1+T')$ is the new threshold, $I_\Phi(z)$ is the interference at z, and the rest of the terms remain unchanged. Recall that the interference at a given location $z \in \mathbb{R}^2$ is given by

$$I_\Phi(z) = \sum_{x_j \in \Phi} L(z, x_j), \text{ with } L(z, x_j) = \frac{h}{l(x_j - z)}, \tag{3}$$

where h is a fading parameter, which is independent of Φ and is defined as an exponential random variable with a mean μ, and $l(x_j - z)$ is the path loss function usually considered to be in a power law form such as $||x_j - z||^\beta$, $(A\max(r_0, ||x_j - z||))^\beta$, or $(1 + ||x_j - z||)^\beta$ where $\beta > 2$ is the path loss exponent and $r_0 > 0$ is a parameter. This model assumes that the user at the given location z connects to the base station (macro or micro base station) closest to it. It should be noted that, for mathematical simplicity, an identical pathloss model is assumed for macro and micro base stations.

The noise W is now given by σ_W^2/P_{Tx}, where the noise power σ_W^2 is assumed to be constant, and P_{Tx} is the transmit power which can be considered as a constant unit power per user. So, for example, if 5 users are connected to a base station then its total transmit power would be $5P_{\text{Tx}}$. Since macro base stations cater to a larger number of users, they have a higher transmit power in total. Though uncommon, this is a simple way to account for different transmit powers of macro and micro base stations. Another method to model different transmit powers for micro and macro base stations is by considering a two point distribution to account for different transmit powers of macro and micro base stations. Though, in this work, we consider the case where P_{Tx} is the unit transmit power per user, it is important to note that the description of the transmit power P_{Tx} is not central to the methods described in this paper, and that altering the assumption (the two point distribution for the transmit power) would not change the methods of analysis documented in this paper in any way – especially since we focus on the interference and consider an interference limited scenario.

A. Notations and Definitions

This section provides further details for our Poisson cluster process model and establishes the main notation used throughout this paper.

Although Section II states that Φ lives in $\mathbb{R}^2$, the Poisson cluster point process model for Φ can be extended to $\mathbb{R}^d$, and we use $\mathbb{R}^d$ in the paragraphs that follow because our results would hold for the general d-dimensional case as well. We shall then restrict the number of dimensions to $d = 2$, as and when required. As before, the cluster centers $\Phi_c \subset \mathbb{R}^d$ form a stationary Poisson process with intensity $\lambda_c > 0$, and we view the cluster member process $\Phi_m \subset \mathbb{R}^d$ as a Neyman-Scott cluster point process specified as follows. Each cluster center $x \in \Phi_c$ triggers a cluster member process $\Phi_m^{(x)} \subset \mathbb{R}^d$, where conditioned on Φ_c, the processes $\Phi_m^{(x)}$ for all $x \in \Phi_c$ are mutually independent and $\Phi_m^{(x)}$ is a Poisson process with intensity function $\lambda_m f(y - x)$ for $y \in \mathbb{R}^d$, which is in agreement with equation (1). Here, $\lambda_m > 0$ is a parameter and f is a density function defined on $\mathbb{R}^d$. We let Φ_m be the superposition of all cluster member processes, i.e. $\Phi_m = \bigcup_{x\in\Phi_c} \Phi_m^{(x)}$. Thereby, conditioned on Φ_c, we have that Φ_m is a Poisson process on $\mathbb{R}^d$ with intensity function $\rho(y) = \lambda_m \sum_{x\in\Phi_c} f(y - x),\ y \in \mathbb{R}^d$.

The notations commonly used in this paper, for locations $x, x', y, \ldots \in \mathbb{R}^d$ and numbers $r > 0$, are:

- $|\cdot| = d$-dimensional Lebesgue measure.
- $\|\cdot\| =$ length in $\mathbb{R}^d$.
- $b(x, r) = \left\{y \in \mathbb{R}^d : ||y - x|| \leq r\right\}$ is the closed ball with center x and radius r.
- o is the origin in $\mathbb{R}^d$.

- An increasing sequence of sampling windows $W_1, W_2, \ldots$ in $\mathbb{R}^d$ will be considered for asymptotic results. Moreover, for $n = 1, 2, \ldots$, we consider the eroded sampling window $W_{n,r} \equiv W_n \ominus b(o,r) = \{x \in W_n : b(x,r) \subseteq W_n\}$.
- δ_x is the Dirac measure at x.
- The clusters that are "added back" to the point process Φ during the use of the Slivnyak-Mecke theorem (see Appendix A) are denoted with a tilde on top and satisfy the following conditions:
  i) $\tilde{\Phi}_m^{(x)}$ for all $x \in \mathbb{R}^d$ are mutually independent and independent of Φ, and
  ii) $\tilde{\Phi}_m^{(x)}$ is distributed as $\Phi_m^{(x)}$.
- A locally finite subset φ of $\mathbb{R}^d$ is called a point configuration, and N_{lf} denotes the set of all point configurations. See Appendix A for details.
- $H(x,r) = \{\varphi \in N_{lf} : \varphi \not\upharpoonright b(x,r)\}$ and $H(x,x',r) = \{\varphi \in N_{lf} : \varphi \not\upharpoonright b(x,r) \cup b(x',r)\}$ are the sets of point configurations which are not r-close to x, and x or x', respectively.
- The probability of Φ_c not being r-close to an arbitrary fixed point in $\mathbb{R}^d$ is

$$v_c(r) \equiv \mathbb{P}\left(\Phi_c \not\upharpoonright b(x,r)\right) = \exp\left(-\lambda_c \left|b(o,r)\right|\right).$$

- The probability of $\Phi_m^{(x)}$ not being r-close to o:

$$v_m(x,r) \equiv \mathbb{P}\left(\Phi_m^{(x)} \not\upharpoonright b(o,r)\right) = \exp\Big(-\lambda_m \int\limits_{\|z\| \le r} f(z-x)\,\mathrm{d}z\Big).$$

  Thus, the probability of $\Phi_m^{(x)}$ not being r-close to y is

$$\mathbb{P}\left(\Phi_m^{(x)} \not\upharpoonright b(y,r)\right) = \exp\Big(-\lambda_m \int\limits_{\|z-y\| \le r} f(z-x)\,\mathrm{d}z\Big) = v_m(x-y,r).$$

  In short, we write $v_m(r) = v_m(o,r)$.
- The void probabilities for Φ are defined by $v(K) \equiv \mathbb{P}\left(\Phi \not\upharpoonright K\right)$ for compact sets $K \subset \mathbb{R}^d$. We have

$$\begin{aligned} v(K) &= \mathbb{P}\left(\Phi_c \not\upharpoonright K, \Phi_m \not\upharpoonright K\right) = \mathbb{E}\left[\mathbf{1}\left(\Phi_c \not\upharpoonright K\right)\mathbb{P}\left(\Phi_m \not\upharpoonright K \,|\, \Phi_c\right)\right] \\ &= \mathbb{E}\left[\prod_{x \in \Phi_c} \mathbf{1}\left(x \notin K\right) \exp\left(-\lambda_m \int\limits_K f(y-x)\mathrm{d}y\right)\right] \\ &= \exp\left(-\lambda_c \int\limits_{\mathbb{R}^d} \left[1 - \mathbf{1}\left(x \notin K\right) \exp\Big(-\lambda_m \int\limits_K f(y-x)\,\mathrm{d}y\Big)\right] \mathrm{d}x\right), \end{aligned}$$

  cf. equation (18) from Appendix A. Thereby,
  1) $v(r) \equiv v(b(o,r))$ is specified by taking $K = b(o,r)$ above;
  2) $v(x,r) \equiv v(b(o,r) \cup b(x,r))$ is specified by taking $K = b(o,r) \cup b(x,r)$ above; notice that $v(b(x,r) \cup b(x',r)) = v(x-x',r)$.
- The probability of $\tilde{\Phi}_m^{(x)}$ not being r-close to x or x' is

$$u_m(x-x',r) \equiv \mathbb{P}\left(\tilde{\Phi}_m^{(x)} \in H(x,x',r)\right) = \exp\left(-\lambda_m \int\limits_{b(x,r) \cup b(x',r)} f(y-x)\,\mathrm{d}y\right)$$

which after substituting $z = y - x$ results in

$$u_m(x - x', r) = \exp\left(-\lambda_m \int\limits_{b(o,r)\cup b(x'-x,r)} f(z)\,\mathrm{d}z\right).$$

- The probability of $\tilde{\Phi}_m^{(y)}$ not being r-close to x or x' is

$$u_m(x - x', y - x', r) \equiv \mathbb{P}\left(\tilde{\Phi}_m^{(y)} \in H(x, x', r)\right) = \exp\left(-\lambda_m \int\limits_{b(x,r)\cup b(x',r)} f(z - y)\,\mathrm{d}z\right)$$

$$= \exp\left(-\lambda_m \int\limits_{b(o,r)\cup b(x'-x,r)} f(z - (y - x'))\,\mathrm{d}z\right).$$

III. Examination of the Interference

This section examines the interference, $I_\Phi(z)$, that a user-base station pair (i.e. a user connected to the base station closest to it, cf. equation (3)) experiences. The most obvious, and intuitive, way to describe interference is to find its distribution or all of its moments. This is done by finding its generating functional or (equivalently) the Laplace functional, because repeated differentiation of the Laplace functional can be used to find the moments of the interference. The Laplace functional of the interference, as shown in [2] and [3], is given by

$$\mathcal{L}_{I_\Phi(z)}(s) = \mathbb{E}\left[\exp\left(-sI_\Phi(z)\right)\right] = \mathbb{E}\left[\prod_{x\in\Phi} \mathcal{L}_h\left(\frac{s}{l(x - z)}\right)\right],$$

where $\mathcal{L}_h\left(s/l(x - z)\right)$ is the Laplace functional of the receive power. Given that the fading h on each link is independent of the point process Φ, and that $h \sim \exp(\mu)$ (Rayleigh fading), we obtain

$$\mathcal{L}_{I_\Phi(z)}(s) = \mathbb{E}\left[\prod_{x\in\Phi}\left(\frac{\mu}{\mu + \frac{s}{l(x-z)}}\right)\right] = \mathbb{E}\left[\prod_{x\in\Phi_c}\left(\frac{\mu}{\mu + \frac{s}{l(x-z)}} \prod_{y\in\Phi_m^{(x)}} \frac{\mu}{\mu + \frac{s}{l(y-z)}}\right)\right].$$

Therefore, conditioning on Φ_c and using equation (18) from Appendix A results in

$$\mathcal{L}_{I_\Phi(z)}(s) = \mathbb{E}\left[\prod_{x\in\Phi_c}\left(\frac{\mu}{\mu + \frac{s}{l(x-z)}} \exp\left(-\lambda_m \int_{\mathbb{R}^d} \frac{\frac{s}{l(y-z)}}{\mu + \frac{s}{l(y-z)}} f(y - x)\mathrm{d}y\right)\right)\right]$$

$$= \exp\left(-\lambda_c \int_{\mathbb{R}^d}\left\{1 - \frac{\mu}{\mu + \frac{s}{l(x-z)}} \exp\left(-\lambda_m \int_{\mathbb{R}^d} \frac{\frac{s}{l(y-z)}}{\mu + \frac{s}{l(y-z)}} f(y - x)\mathrm{d}y\right)\right\}\mathrm{d}x\right). \quad (4)$$

A. Utility of the Finding

One of our research objectives is to be able to find a framework that is independent of the exact deployment topology (such as assuming a uniform hexagonal grid) which allows us to ascertain important performance indicators, such as probability of coverage, spectral efficiency, etc. The use of this framework results in relationships between user intensity, base station intensity, system parameters (such as transmit power, pathloss, etc.), and the performance indicators. It enables us to gage the effectiveness of HetNets over large areas, such as states or countries, where networks of different topologies are deployed in various localities. Such a framework can then be used to solve various optimization problems related to capital expenditure, operational expenditure, energy efficiency, etc. It would also help facilitate the design of strategies to manage and improve such networks.

1) Probability of Coverage: In this section, for computational simplicity, we assume that $d = 2$. Denote $p(\lambda_c, \lambda_m, f(\cdot), T, \beta \,|\, R)$ as the conditional probability that a user at an arbitrary location is covered by the nearest base station at a distance R, for a particular pathloss exponent and threshold. By stationarity of Φ, we can assume that the user is located at o, and hence, R is the random distance from o to the nearest point (i.e. base station) in Φ. Let g denote the continuous density function of R. Then, the probability of coverage in an area for the *interference limited case*[5] is given by

$$p\left(\lambda_c, \lambda_m, f(\cdot), T, \beta\right) \equiv \mathbb{E}\big[\mathbb{P}\left\{\text{SIR} \geq T \,|\, r\right\}\big] = \int \mathbb{P}\left\{\text{SIR} \geq T \,|\, r\right\} g(r)\mathrm{d}r.$$

We find that $g(r) = \frac{\mathrm{d}}{\mathrm{d}r}\mathbb{P}\left(\Phi \uparrow b\left(o, r\right)\right) = -\frac{\mathrm{d}}{\mathrm{d}r}v(r)$. Further, assume that $l(x_i) = l(R)$ depends only on the distance from the user at o to its nearest station x_i (as is usually the case in examples of applications). Now, recalling that $h \sim \exp(\mu)$ is independent of Φ and that $\text{SIR} = L(o, x_i)/I_\Phi(o)$, for any realization $R = r$, we get

$$\begin{aligned} p\left(\lambda_c, \lambda_m, f(\cdot), T, \beta \,|\, r\right) &\equiv \mathbb{P}\{\text{SIR} \geq T \,|\, r\} = \mathbb{P}\left\{h \geq l(r) T I_\Phi(o) \,|\, r\right\} \\ &= \mathbb{E}\big[\exp\left(-\mu l(r) T I_\Phi(o)\right) \,|\, r\big] = \mathcal{L}_{I_\Phi(o)}(\mu l(r) T). \end{aligned}$$

Hence, the conditional probability of coverage can be written as

$$p\left(\lambda_c, \lambda_m, f(\cdot), T, \beta \,|\, r\right) = \exp\left(-\lambda_c \int_{\mathbb{R}^2} \left\{1 - \frac{\mu}{\mu + \frac{\mu l(r) T}{l(x)}} \exp\left(-\lambda_m \int_{\mathbb{R}^2} \frac{\frac{\mu l(r) T}{l(y)}}{\mu + \frac{\mu l(r) T}{l(y)}} f(y - x)\mathrm{d}y\right)\right\} \mathrm{d}x\right). \tag{5}$$

Therefore[6],

$$\begin{aligned} &p\left(\lambda_c, \lambda_m, f(\cdot), T, \beta\right) = \\ &\int_{\mathbb{R}^+} \exp\left(-\lambda_c \int_{\mathbb{R}^2} \left\{1 - \frac{\mu}{\mu + \frac{\mu l(r) T}{l(x)}} \exp\left(-\lambda_m \int_{\mathbb{R}^2} \frac{\frac{\mu l(r) T}{l(y)}}{\mu + \frac{\mu l(r) T}{l(y)}} f(y - x)\mathrm{d}y\right)\right\} \mathrm{d}x\right) g(r)\,\mathrm{d}r. \end{aligned} \tag{6}$$

For instance, assuming the cluster distribution $f(\cdot)$ to be the density of a zero-mean radially symmetric Gaussian with variance σ^2, integrating equations (5) and (6) numerically allows us to observe the variations in the probability of coverage based on a pair of parameters, while all the others are kept fixed. The pathloss function is considered to be of the form $l(r) = (1 + r)^\beta$ and the pathloss exponent β is equal to 4. Since there are many input parameters, they are dealt with in pairs and lead to the following observations.

Fig. 2 depicts changes in the conditional probability of coverage when the distance between any given user and base station pair is varied for different micro base station intensities while keeping all other parameters constant. Overall, the conditional probability of coverage decreases as the average intensity of micro base stations around a macro base station increases. This is due to an increase in the amount of inter- and intra- cluster interference experienced by a user in the area which causes the ratio of receive power to interference power to fall below the threshold value, and thereby, results in coverage holes. The curve for $\lambda_m = 1$ forms (a sort of) an upper boundary for the conditional probability of coverage due to the fact that this case has the lowest intra-cluster interference. For higher micro base station intensities, it is interesting to observe that the probability of coverage increases when the distance between a user and base station pair is between $0.5 - 1.75$ km and then decreases as expected. This is because the user base station distance is quite large, which implies that the rest of the points within the cluster are farther away

[5]For HetNets, the interference limited scenario (where the effects of the interference dominate) is considered to be more appropriate due to very dense base station deployments. Therefore, the effects of noise are neglected, i.e., $\sigma_W^2 = 0$.

[6]Note that μ cancels out in both equations (5) and (6), i.e. we can, e.g., take $\mu = 1$ in (5) and (6).

and so are the base stations in other clusters[7]. This results in lower intra- and inter- cluster interference, and thereby, an increase in the conditional probability of coverage. However beyond a certain distance (> 2.0 km), regardless of the intensity of micro base stations considered, the probability of coverage decreases at a uniform rate because the ratio of receive power to interference power falls below the threshold. Note that the micro base station intensities considered in Fig. 2 are far larger than in other figures. This is to ensure that, as far as the conditional probability of coverage is concerned, there is no significant added benefit even when micro base station intensities are extremely large.

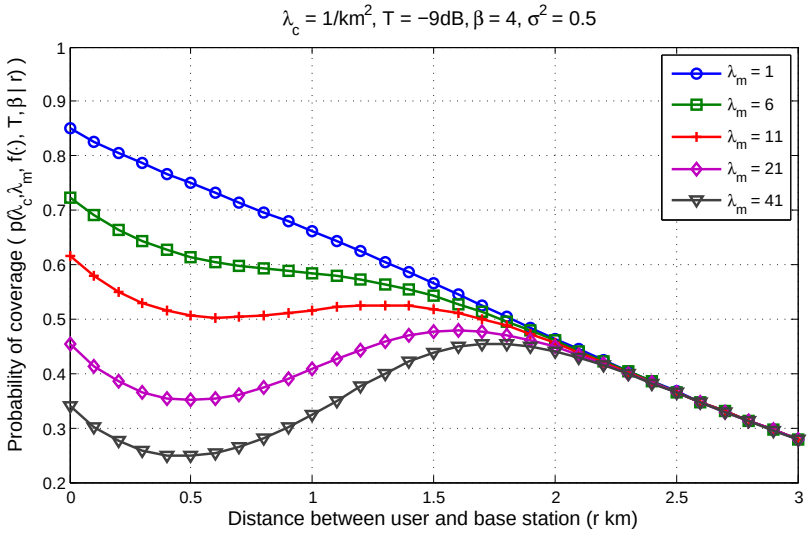

Fig. 2. Conditional probability of coverage vs. distance for various micro base station intensities.

Fig. 3 plots the conditional probability of coverage against various thresholds for selected micro base station intensities. Intuitively, higher the threshold, lower the probability of coverage. An important aspect highlighted by the figure is that, an increase in the number of micro base stations causes a corresponding increase in the intra-cluster interference which results in a sharp decline in the conditional probability of coverage.

Fig. 4(a) and Fig. 4(b) depict changes in the conditional probability of coverage when the variance of the cluster distribution is altered for different micro base station intensities. A cursory comparison of the figures shows that the distance between the user and base station also plays a role in determining the conditional probability of coverage. However, though a smaller distance between the user and base station results in a higher conditional probability of coverage, it is important to note that the fundamental shape of the curves remain unchanged. For very small variance values, the probability of coverage decreases sharply due to extremely high intra-cluster interference. The effect of intra-cluster interference decreases as the variance increases resulting in a significant increase in the probability of coverage. Note that, as $\sigma^2 \to 0$, the conditional probability of coverage is significantly higher (similar to a homogeneous network, see Fig. 6 in [1]) because $f(\cdot)$ in equation (5) tends to a Dirac delta function which implies that the micro base stations are at the same location as the macro base station, and can therefore, be considered similar to a homogeneous wireless network where base stations have multiple transmit antennas.

Finally, Fig. 5 shows the plot of the coverage probability in a given area (from equation (6)) for increasing micro base station intensities when the other parameters are fixed. For a particular macro base station intensity, this plot shows that increasing the micro base station intensity does not increase the coverage probability significantly ($\approx 10\%$ increase). It is also interesting to note that, for a given micro base station intensity, the coverage probability decreases as the macro base station intensity increases. This decrease is due to an increase in interference power in the area which in turn requires the receive

[7]This is because we assume that the user connects to the nearest base station.

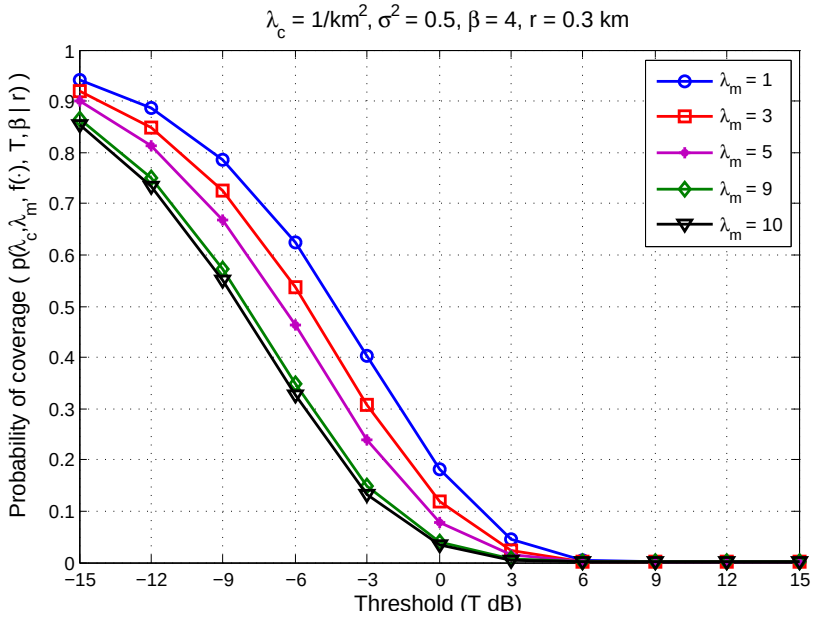

Fig. 3. Conditional probability of coverage vs. threshold for various micro base station intensities.

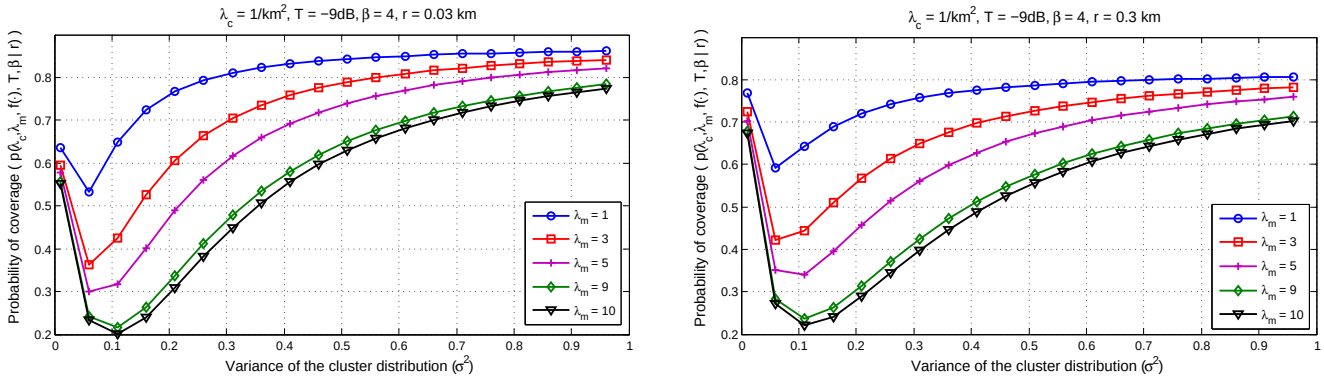

(a) User to base station distance, $r = 0.03$ km.

(b) User to base station distance, $r = 0.3$ km.

Fig. 4. Conditional probability of coverage vs. variance of the cluster distribution for various micro base station intensities.

power to be much larger in order to overcome the restriction imposed by the threshold. Therefore, it is reasonable to conclude that micro base station deployments are probably better suited for improving individual user throughputs rather than improving overall coverage in the area.

2) Spatially Averaged Rate: The spatially averaged rate or spectral efficiency, for the interference limited scenario, is given by

$$\bar{R}_{\Phi}\left(\lambda_c, \lambda_m, f(\cdot), \beta\right) = \int_{\mathbb{R}} p\left(\lambda_c, \lambda_m, f(\cdot), (e^T - 1), \beta\right) \mathrm{d}T, \tag{7}$$

where $p\left(\cdot\right)$ is substituted from equation (6). Note that further numerical analysis has not been included to ensure brevity of the work.

IV. Asymptotic Behavior of the Interference

An alternate method of describing the interference experienced by a user who is at a distance r from its nearest base station, $I_{\Phi}(r)$, is by observing its asymptotic behavior. Since describing the interference in the whole area ($\mathbb{R}^d$) is rather complicated, we estimate the interference over smaller subsets of the area

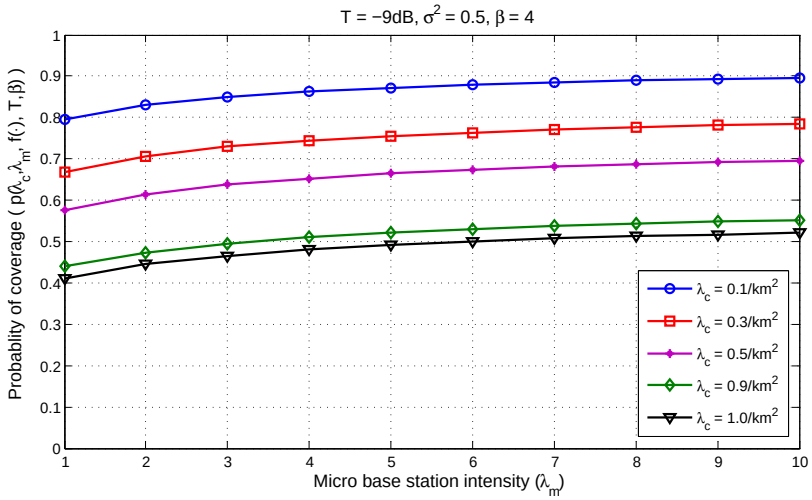

Fig. 5. Coverage probability vs. micro base station intensities for various macro base station intensities.

(sampling windows). The asymptotic behavior of the interference is studied using an increasing sequence of compact sampling windows[8] $(W_n)_{n\geq 1}$ in $\mathbb{R}^d$, and eroded sets $W_{n,r}$ which for technical reasons satisfy the *Regularity Condition*[9]. The estimator of the interference, $S(r) = I_\Phi(r)$, is defined by

$$S_n(r) = \frac{1}{|W_{n,r}|} \sum_{x\in\Phi} \mathbf{1}_{W_{n,r}}(x)\mathbf{1}_{H(x,r)}(\Phi - \delta_x).$$

Note that we can identify Φ with locally finite counting measures without multiplicities, cf. Appendix A. This observation becomes convenient in the calculations in the sequel where we simply write Φ instead of the more cumbersome notation $\sum_{x\in\Phi}\delta_x$ for the corresponding counting measure. Now, a centered random variable, $Z_n(r)$, is constructed from the estimator as

$$Z_n(r) = \left(|W_{n,r}|\right)^{1/2}\left(S_n(r) - \mathbb{E}\left[S_n(r)\right]\right).$$

Then, we have the following theorem, where a rigorous proof (based on [5]) has been elucidated in [14].

Theorem 1. *For any radius $r \geq 0$, such that $\lim_{n\to\infty} Var\left[Z_n(r)\right] = \sigma^2_\lambda(r) > 0$, we have*

$$Z_n(r) \xrightarrow[n\to\infty]{D} \mathcal{N}(0, \sigma^2_\lambda(r))$$

where $\mathcal{N}(0, \sigma^2_\lambda(r))$ is a zero-mean Gaussian distribution with variance $\sigma^2_\lambda(r)$.

Significance of the findings: Theorem 1 shows that the interference for heterogeneous networks with two types of base stations can be approximated by a Gaussian distribution with mean $\mathbb{E}\left[S_n(r)\right]$ and variance $|W_{n,r}|\sigma^2_\lambda(r)$. It is important to note that, the description of interference as a Gaussian random variable remains unchanged regardless of functionals such as transmit power, fading, pathloss, etc. that are attributed to these points (base stations). This result, therefore, implicitly holds for all pathloss exponents $\beta > 2$. The influence of the functionals can be observed solely in the mean and variance of the interference. Hence, finding the mean and the variance of the estimator will complete the description of the interference. However, it is also important to note that choosing pathloss functionals that avoid singularities greatly simplifies computations of the mean and variance.

[8]Note: The sampling windows cover all of $\mathbb{R}^d$ in the limit.

[9]Please see [14] for the precise definition of the Regularity Condition and its utility. [14] also contains references that specify unbiased estimators similar to the one defined in this paper.

A. Finding the Mean and Variance of the Estimator

Fundamentally, the interference as described by equation (3), comprises of three independent components – transmit power, fading, and pathloss. Out of the three, only one of them (namely, the pathloss) is a function dependent on the points Φ (i.e. the base stations). From Section II, we observe that the pathloss is essentially dependent on the distance between a given user location and the location of a given base station (a point of Φ). In its simplest form, the pathloss is a function of the distance in power law form and the pathloss exponent is a constant greater than 2, i.e. $\beta > 2$. Based on this observation, we can use void probabilities or the probability that no other point of the point process is within a distance r of any user and base station pair. This subsection uses the notations for the void probabilities detailed in Section II-A to describe the mean and the variance.

1) The Mean:

$$\mathbb{E}\left[S_n(r)\right] = \frac{1}{|W_{n,r}|}\mathbb{E}\left[\sum_{x\in\Phi} \mathbf{1}_{W_{n,r}}(x)\mathbf{1}_{H(x,r)}(\Phi - \delta_x)\right]. \tag{8}$$

Appendix B details the derivation of equation (17), which when divided by $|W_{n,r}|$, gives the mean of the estimator as

$$\mathbb{E}\left[S_n(r)\right] = \lambda_c v(r)\left[v_m(r) + \lambda_m \int\limits_{\|z\|>r} v_m(z,r) f(z)\mathrm{d}z\right]. \tag{9}$$

2) The Variance:

$$\sigma^2_\lambda(r) = \mathrm{Var}\left(S_n(r)\right) = \frac{1}{|W_{n,r}|^2}\mathrm{Var}\left(\left[\sum_{x\in\Phi} \mathbf{1}_{W_{n,r}}(x)\mathbf{1}_{H(x,r)}(\Phi - \delta_x)\right]\right). \tag{10}$$

As shown in Appendix C,

$$\mathrm{Var}\left(S_n(r)\right) = \frac{1}{|W_{n,r}|^2}\Big[\xi_{CC}(r) \;+\; 2\left(\xi_{CM}(r) + \xi_{CCM}(r)\right) + \xi_{CMM}(r) + \xi_{CCMM}(r) + \xi_M(r) - \left\{\xi_M(r)\right\}^2\Big], \tag{11}$$

where

$$\xi_{CC}(r) = \lambda_c^2 \int\limits_{\|z\|>r} |W_{n,r} \cap (W_{n,r} + z)|\, v(z,r)\, (u_m(z,r))^2 \mathrm{d}z, \tag{12}$$

$$\xi_{CM}(r) = \lambda_c\lambda_m \int\limits_{\|z\|>r} |W_{n,r} \cap (W_{n,r} + z)|\, v(z,r)\, u_m(z,r)\, f(z)\mathrm{d}z, \tag{13}$$

$$\xi_{CCM}(r) = \lambda_c^2\lambda_m \iint\limits_{\substack{\|z-w\|>r \\ \|z\|>r \\ \|w\|>r}} |W_{n,r} \cap (W_{n,r} + z)|\, v(z,r)\, u_m(z,r)\, u_m(z,w,r)\, f(w)\, \mathrm{d}z\, \mathrm{d}w, \tag{14}$$

$$\xi_{CMM}(r) = \lambda_c\lambda_m^2 \iint\limits_{\substack{\|z\|>r \\ \|w\|>r \\ \|z-w\|>r}} |W_{n,r} \cap (W_{n,r} + w - z)|\, v(w-z,r)\, u_m(w-z,w,r) \, f(z)\, f(w)\, \mathrm{d}z\, \mathrm{d}w, \tag{15}$$

$$\xi_{CCMM}(r) = \lambda_c^2 \lambda_m^2 \iiint\limits_{\substack{\|w\|>r \\ \|z\|>r \\ \|w+z'\|>r \\ \|z-w\|>r \\ \|z'\|>r \\ \|z+z'-w\|>r}} |W_{n,r} \cap (W_{n,r}+w)|\, v(w,r)\, u_m(w, w-z, r) \, u_m(w, -z', r)\, f(z)\, f(z')\, \mathrm{d}w\, \mathrm{d}z\, \mathrm{d}z', \tag{16}$$

and

$$\xi_M(r) = \lambda_c\, |W_{n,r}|\, v(r) \left[v_m(r) + \lambda_m \int\limits_{\|z\|>r} v_m(z,r) f(z) \mathrm{d}z \right]. \tag{17}$$

B. Validation of the Asymptotic Behavior

This section contains simulations results that show the validity of the findings of Section IV, which details the asymptotic behavior of the interference. First, we validate the convergence result based on system level simulations of a mobile network consisting of base stations distributed according to a Poisson cluster process with omni-directional antennas. The system level simulation computes the interference experienced by user and base station pairs (in a HetNet), assuming that the user connects to the base station from which the maximum receive power is obtained. The receive power at a user location, and determination of the base station to which it connects, is based on a pathloss exponent equal to 4 (i.e. $\beta = 4$) and Rayleigh fading. The threshold is set at -5 dB according to the SINR threshold applied in 4G-LTE verification[10]. The simulation also assumes that the average number of micro base stations deployed depends on the user density in the area; i.e. larger the number of users, larger the average number of micro base stations realized per macro base station. The variance of the distribution of the micro base stations around the macro base station σ^2 is set at 0.5 to ensure that micro base stations are fairly widely spread out. Fig. 6 shows that the interference experienced by a user (connected to its nearest base station) is indeed Gaussian distributed. This phenomenon was observed consistently when simulations were carried out for various base station realizations as well as for varying user and base station distances. Thus, validating the theorem in Section IV.

Fig. 7 compares normalized values of the mean of the interference averaged over various user–base station distances. The expression for the mean of the interference matches the values obtained by simulations quite closely, especially for high base station intensities. This illustrates that this model, though simplistic, can prove to be quite accurate in describing the mean interference in such complex networks. Both theory and simulations indicate that interference increases as the base station intensities increase, which concurs with the observation in Fig. 2 where the conditional probability of coverage decreases due an increase in the interference.

Fig. 8 compares normalized values of the variance of the interference averaged over various user–base station distances. The curves obtained by simulation and theory are fairly similar, though they are not an exact match as seen in the case of the mean. The curves for $\lambda_c = 2/\mathrm{km}^2$ are particularly close. The discrepancy in the curves is due to the fact that the number of Monte-Carlo simulations (though large) were insufficient to obtain more accurate values. However, it is interesting to note that as the base station intensities increase, both sets of curves indicate that the deviation of the values of the interference away from its mean is extremely small. Therefore, for certain optimization problems, the use of the mean of the interference should suffice.

C. Utility of the Findings

The asymptotic convergence of the interference to a Gaussian distribution greatly simplifies the amount of effort required to compute the probability of coverage or spectral efficiency as given by equations (5)

[10]Taken from Annex A Section A.1 of 3gpp TR 36.942 Evolved Universal Terrestrial Radio Access (E-UTRA); Radio Frequency (RF) system scenarios, http://www.3gpp.org/ftp/Specs/html-info/36942.htm

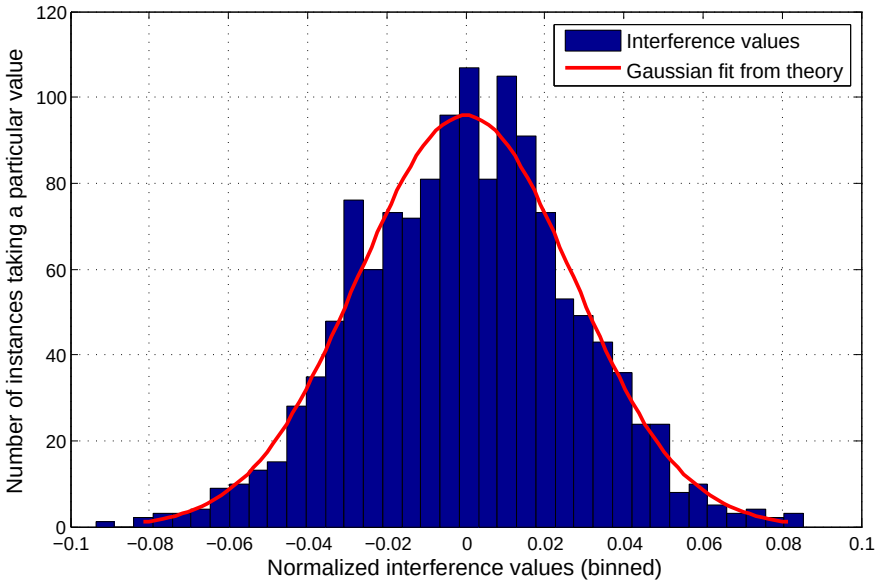

Fig. 6. Histogram for simulated interference values and the Gaussian density with the mean and variance calculated from equations (9) and (11).

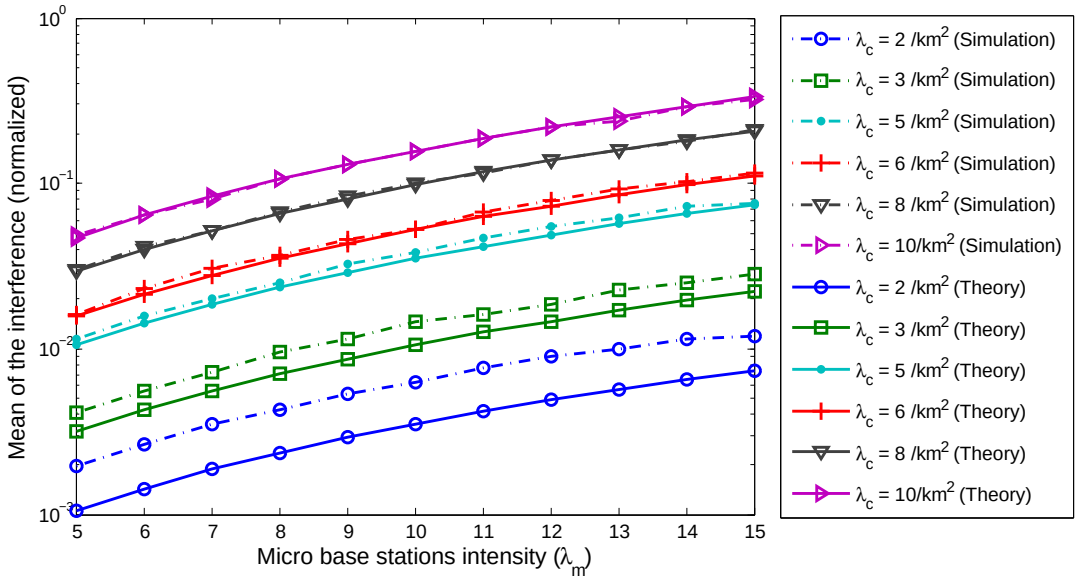

Fig. 7. Theoretic mean (solid lines) versus mean calculated using simulations (dashed lines).

and (7), respectively. By using the expressions for the mean and variance of the interference derived in Section IV-A, the exponential term in equation (5) which is rather complicated can be replaced by a much simpler (Gaussian) term. This makes it easier to optimize such complicated networks with performance indicators as constraints. It is important to note that, though the expressions for mean and variance appear rather large and cumbersome, solving them numerically is something that is quite easily done.

V. Conclusion

This paper models a HetNet using a Poisson cluster process model and examines the interference experienced by a user in such a network. The main contributions of this work are a complete description of the interference, and expressions for the mean and variance of the estimator of the interference whose convergence to a Gaussian distribution was shown in [14]. The veracity of the theoretic findings have been

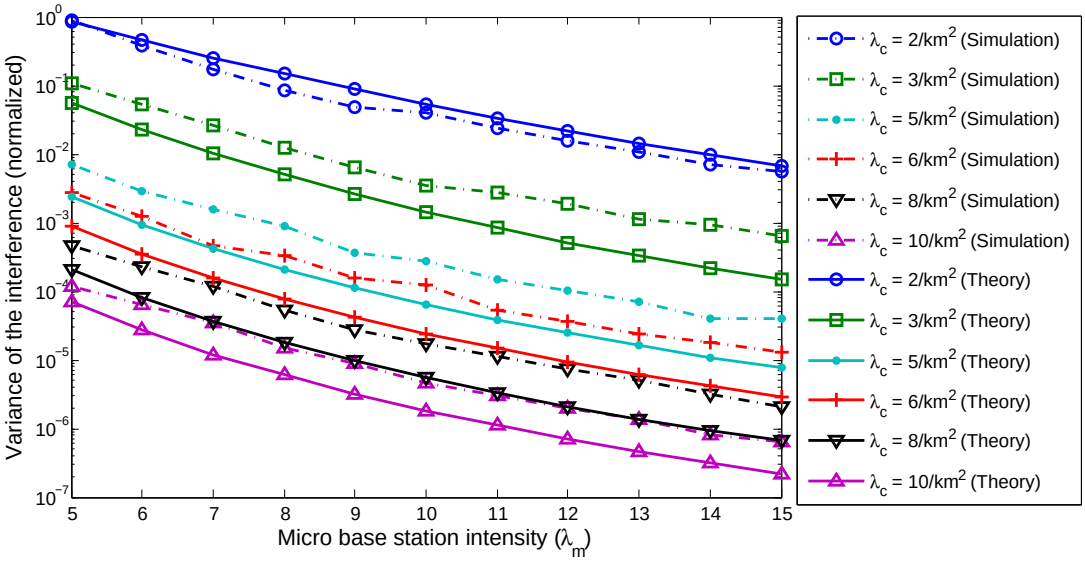

Fig. 8. Theoretic variance (solid lines) versus variance calculated using simulations (dashed lines).

corroborated by simulations. These findings allow us to understand the behavior of such complex networks, while saving a lot of time and effort that is required for simulation. They also simplify computations of key system parameters such as the probability of coverage and enable easier re-use in other problems geared towards calculating and optimizing the efficiency and efficacy of such networks.

APPENDIX A
IMPORTANT THEOREMS

For any subset $x \subseteq A$, let $n(x)$ denote the cardinality of x, setting $n(x) = \infty$ if x is not finite, and for any $B \subset \mathbb{R}^d$, let $x_B = x \cap B$ be the restriction of x to B. Recall that x is locally finite if $n(x_B) < \infty$ whenever $B \subset \mathbb{R}^d$ is bounded, and we shall then refer to x as a point configuration. Denote the space of point configurations by

$$N_{lf} = \left\{x \subseteq \mathbb{R}^d : n(x_B) < \infty \text{ for all bounded } B \subset \mathbb{R}^d\right\}.$$

Note that N_{lf} can be identified by the set of locally finite counting measures without multiplicities.

A locally finite spatial point process on $\mathbb{R}^d$ without multiple points can be viewed as a random countable subset $X \subset \mathbb{R}^d$, i.e. X takes values in N_{lf} (for further details, see [11]). Thus X can be identified with the counting process given by $N = \sum_{x \in X} \delta_x$. For simplicity, we write X for N. It will always be clear from the context whether we view X as a random set or a counting process. For the following two results, $X \subset \mathbb{R}^d$ is assumed to be a Poisson process with intensity function ζ. The results are verified in [11].

Poisson Generating Functional for a Poisson process. *For any Borel function* $k : \mathbb{R}^d \mapsto [0, 1]$,

$$\mathbb{E}\left[\prod_{x \in X} k(x)\right] = \exp\left(-\int_{\mathbb{R}^d} (1 - k(x))\zeta(x)\,\mathrm{d}x\right). \tag{18}$$

Slivnyak-Mecke Theorem for a Poisson process. *For any non-negative measurable function* h *defined on* $\mathbb{R}^d \times N_{lf}$,

$$\mathbb{E}\sum_{x \in X} h(x, X - \delta_x) = \int_{\mathbb{R}^d} \mathbb{E}h(x, X)\,\zeta(x)\mathrm{d}x$$

The Slivnyak-Mecke Theorem above can be extended to very general Poisson processes, including marked Poisson processes (see [6]) and in particular the marked Poisson process $\{(x, \Phi_m^{(x)}) : x \in \Phi_c\}$.

Thereby, we obtain the following Slivnyak-Mecke Theorem for the Poisson cluster process Φ, and by iterative use of this result, the following Extended Slivnyak-Mecke Theorem for Φ is derived.

Slivnyak-Mecke Theorem for Φ. *For any non-negative measurable function h defined on $\mathbb{R}^d \times N_{lf} \times N_{lf}$,*

$$\mathbb{E} \sum_{x \in \Phi_c} h(x, \Phi_m^{(x)}, \Phi - \delta_x) = \lambda_c \int \mathbb{E} h(x, \tilde{\Phi}_m^{(x)}, \Phi + \tilde{\Phi}_m^{(x)}) \, \mathrm{d}x.$$

Extended Slivnyak-Mecke Theorem for Φ. *For any non-negative measurable function h defined on $\mathbb{R}^d \times \mathbb{R}^d \times N_{lf} \times N_{lf} \times N_{lf}$,*

$$\mathbb{E} \sum_{x, x' \in \Phi_c}^{\neq} h(x, x', \Phi_m^{(x)}, \Phi_m^{(x')}, \Phi - \delta_x) = \lambda_c^2 \int \int \mathbb{E} h(x, x', \tilde{\Phi}_m^{(x)}, \tilde{\Phi}_m^{(x')}, \Phi + \tilde{\Phi}_m^{(x)} + \tilde{\Phi}_m^{(x')} + \delta_{x'}) \, \mathrm{d}x \, \mathrm{d}x'$$

where $\neq$ over the summation sign means $x \neq x'$.

APPENDIX B
DERIVATION OF THE MEAN

The RHS of the equation (8) can be derived as follows:

$$\begin{aligned} \xi_M(r) \equiv |W_{n,r}| \mathbb{E}\left[S_n(r)\right] &= \mathbb{E}\left[\sum_{x \in \Phi} \mathbf{1}_{W_{n,r}}(x) \mathbf{1}_{H(x,r)}(\Phi - \delta_x)\right] \\ &= \mathbb{E} \sum_{x \in \Phi_c} \left[\mathbf{1}_{W_{n,r}}(x) \mathbf{1}_{H(x,r)}(\Phi - \delta_x) + \sum_{y \in \Phi_m^{(x)}} \mathbf{1}_{W_{n,r}}(y) \mathbf{1}_{H(y,r)}(\Phi - \delta_y)\right]. \end{aligned}$$

Using the Slivnyak-Mecke Theorem for Φ (Appendix A), we get

$$\begin{aligned} \xi_M(r) = \lambda_c \int_{W_{n,r}} \mathbb{E}\left[\mathbf{1}_{H(x,r)}\left(\Phi + \tilde{\Phi}_m^{(x)}\right)\right] \mathrm{d}x + \\ \lambda_c \int \mathbb{E}\left[\sum_{y \in \Phi_m^{(x)}} \mathbf{1}_{W_{n,r}}(y) \mathbf{1}_{H(y,r)}(\Phi + \tilde{\Phi}_m^{(x)} + \delta_x - \delta_y)\right] \mathrm{d}x \end{aligned}$$

since Φ and $\tilde{\Phi}_m^{(x)}$ are independent. The use of the Slivnyak-Mecke theorem for the process $\Phi_m^{(x)}$, after conditioning on both $\Phi - \Phi_m^{(x)}$ and $\tilde{\Phi}_m^{(x)}$, results in

$$\begin{aligned} \xi_M(r) = \lambda_c \int_{W_{n,r}} \mathbb{E}\left[\mathbf{1}_{H(x,r)}(\Phi) \mathbf{1}_{H(x,r)}(\tilde{\Phi}_m^{(x)})\right] \mathrm{d}x + \\ \lambda_c \lambda_m \iint_{||x-y|| > r} \mathbf{1}_{W_{n,r}}(y) \, \mathbb{P}\left(\Phi \in H(y,r)\right) \, \mathbb{P}\left(\tilde{\Phi}_m^{(x)} \in H(y,r)\right) \, f(x-y) \, \mathrm{d}y \, \mathrm{d}x, \end{aligned}$$

which implies

$$\xi_M(r) = \lambda_c \, |W_{n,r}| \, v(r) \, v_m(r) + \lambda_c \lambda_m \iint_{||x-y|| > r} \mathbf{1}_{W_{n,r}}(y) \, v(r) \, v_m(x-y, r) \, f(x-y) \mathrm{d}y \, \mathrm{d}x.$$

Thereby, equation (17) is obtained by a simple change of variables.

APPENDIX C
DERIVATION OF THE VARIANCE

Observe that $|W_{n,r}|^2 \operatorname{Var}(S_n(r))$ is equal to

$$\operatorname{Var}\left(\left[\sum_{x\in\Phi} \mathbf{1}_{W_{n,r}}(x)\mathbf{1}_{H(x,r)}(\Phi-\delta_x)\right]\right) = \mathbb{E}\left[\sum_{x,x'\in\Phi}^{\neq} \mathbf{1}_{W_{n,r}}(x)\mathbf{1}_{H(x,r)}(\Phi-\delta_x)\,\mathbf{1}_{W_{n,r}}(x')\,\mathbf{1}_{H(x',r)}(\Phi-\delta_{x'})\right] + \mathbb{E}\left[\sum_{x\in\Phi} \mathbf{1}_{W_{n,r}}(x)\mathbf{1}_{H(x,r)}(\Phi-\delta_x)\right] - \left\{\mathbb{E}\left[\sum_{x\in\Phi} \mathbf{1}_{W_{n,r}}(x)\mathbf{1}_{H(x,r)}(\Phi-\delta_x)\right]\right\}^2. \quad (19)$$

The middle term and the last term of the equation are similar to the mean, and have been shown to be equal to equation (17). The first term of equation (19) needs to be derived considering five different scenarios which are detailed as follows:

1) If x, x' belong to the process of cluster centers, the first term of equation (19) is

$$\begin{aligned}
\xi_{CC}(r) &\equiv \mathbb{E}\left[\sum_{x,x'\in\Phi_c}^{\neq} \mathbf{1}_{W_{n,r}}(x)\,\mathbf{1}_{H(x,r)}(\Phi-\delta_x)\,\mathbf{1}_{W_{n,r}}(x')\,\mathbf{1}_{H(x',r)}(\Phi-\delta_{x'})\right] \\
&\overset{(a)}{=} \lambda_c^2 \int_{W_{n,r}}\int_{W_{n,r}} \mathbb{E}\big[\mathbf{1}_{H(x,r)}\left(\Phi+\tilde{\Phi}_m^{(x)}+\tilde{\Phi}_m^{(x')}+\delta_{x'}\right)\mathbf{1}_{H(x',r)}\left(\Phi+\tilde{\Phi}_m^{(x)}+\tilde{\Phi}_m^{(x')}+\delta_x\right)\big]\,\mathrm{d}x\,\mathrm{d}x' \\
&\overset{(b)}{=} \lambda_c^2 \int_{W_{n,r}} \int_{\substack{W_{n,r}\\ \|x-x'\|>r}} \mathbb{P}\left(\Phi\in H(x,x',r)\right)\mathbb{P}\left(\tilde{\Phi}_m^{(x)}\in H(x,x',r)\right)\mathbb{P}\left(\tilde{\Phi}_m^{(x')}\in H(x,x',r)\right)\mathrm{d}x\,\mathrm{d}x' \\
&= \lambda_c^2 \int_{W_{n,r}} \int_{\substack{W_{n,r}\\ \|x-x'\|>r}} v(x-x',r)\,u_m(x-x',r)\,u_m(x'-x,r)\,\mathrm{d}x\,\mathrm{d}x'
\end{aligned}$$

where (a) is obtained using the Extended Slivnyak-Mecke Theorem for Φ (Appendix A), and (b) follows from the independence of $\Phi, \tilde{\Phi}_m^{(x)}$, and $\tilde{\Phi}_m^{(x')}$. Then substitute $x-x'=z$. If $f(\cdot)$ is symmetric, then $u_m(z,r)=u_m(-z,r)$, and thereby, we get equation (12).

2) If x belongs to the cluster center process and x' belongs to the cluster member process triggered by x, then we have

$$\begin{aligned}
\xi_{CM}(r) &\equiv \mathbb{E}\left[\sum_{x\in\Phi_c}\sum_{x'\in\Phi_m^{(x)}} \mathbf{1}_{W_{n,r}}(x)\,\mathbf{1}_{H(x,r)}(\Phi-\delta_x)\,\mathbf{1}_{W_{n,r}}(x')\,\mathbf{1}_{H(x',r)}(\Phi-\delta_{x'})\right] \\
&\overset{(a)}{=} \lambda_c \int_{W_{n,r}} \mathbb{E}\left[\sum_{x'\in\tilde{\Phi}_m^{(x)}} \mathbf{1}_{H(x,r)}(\Phi+\tilde{\Phi}_m^{(x)})\,\mathbf{1}_{W_{n,r}}(x')\,\mathbf{1}_{H(x',r)}(\Phi+\tilde{\Phi}_m^{(x)}+\delta_x-\delta_{x'})\right]\mathrm{d}x \\
&\overset{(b)}{=} \lambda_c\lambda_m \int_{W_{n,r}} \int_{\substack{W_{n,r}\\ \|x-x'\|>r}} \mathbb{P}\left(\Phi\in H(x,x',r)\right)\mathbb{P}\left(\tilde{\Phi}_m^{(x)}\in H(x,x',r)\right) f(x'-x)\mathrm{d}x\,\mathrm{d}x' \\
&= \lambda_c\lambda_m \int_{W_{n,r}} \int_{\substack{W_{n,r}\\ \|x-x'\|>r}} v(x-x',r)\,u_m(x'-x,r) f(x'-x)\mathrm{d}x\,\mathrm{d}x',
\end{aligned}$$

where (a) is obtained using the Slivnyak-Mecke Theorem for Φ, and (b) is obtained by conditioning on Φ and using the Slivnyak-Mecke Theorem for $\tilde{\Phi}_m^{(x)}$. Thereby, equation (13) is obtained by a change of variables and because $v(x-x',r) = v(x'-x,r)$.

3) When x belongs to the cluster center process and x' belongs to the cluster member process triggered by another cluster center, we get

$$\xi_{CCM}(r) \equiv \mathbb{E}\left[\sum_{x\in\Phi_c}\sum_{y\in\Phi_c\setminus\{x\}}\sum_{x'\in\Phi_m^{(y)}} \mathbf{1}_{W_{n,r}}(x)\,\mathbf{1}_{H(x,r)}(\Phi-\delta_x)\,\mathbf{1}_{W_{n,r}}(x')\,\mathbf{1}_{H(x',r)}(\Phi-\delta_{x'})\right].$$

Then, using the extended Slivnyak-Mecke Theorem for Φ results in

$$\xi_{CCM}(r) = \lambda_c^2\int\int \mathbf{1}_{W_{n,r}}(x)\,\mathbb{E}\Big[\sum_{x'\in\tilde{\Phi}_m^{(y)}} \mathbf{1}_{H(x,r)}(\Phi+\tilde{\Phi}_m^{(x)}+\tilde{\Phi}_m^{(y)}+\delta_y)\,\mathbf{1}_{W_{n,r}}(x')$$
$$\mathbf{1}_{H(x',r)}(\Phi+\tilde{\Phi}_m^{(x)}+\tilde{\Phi}_m^{(y)}+\delta_x+\delta_y-\delta_{x'})\Big]\mathrm{d}x\,\mathrm{d}y.$$

Since $\Phi, \tilde{\Phi}_m^{(x)}$, and $\tilde{\Phi}_m^{(y)}$ are independent, by conditioning on $\Phi, \tilde{\Phi}_m^{(x)}$ and using the Slivnyak-Mecke Theorem for $\tilde{\Phi}_m^{(y)}$, we obtain

$$\xi_{CCM}(r) = \lambda_c^2\lambda_m \iiint\limits_{\substack{\|x-y\|>r\\ \|x-x'\|>r\\ \|x'-y\|>r}} \mathbf{1}_{W_{n,r}}(x)\,\mathbf{1}_{W_{n,r}}(x')\,\mathbb{P}\left(\Phi\in H(x,x',r)\right)\mathbb{P}\left(\tilde{\Phi}_m^{(x)}\in H(x,x',r)\right)$$
$$\mathbb{P}\left(\tilde{\Phi}_m^{(y)}\in H(x,x',r)\right) f(y-x')\mathrm{d}x'\,\mathrm{d}y\,\mathrm{d}x$$

$$= \lambda_c^2\lambda_m \iiint\limits_{\substack{\|x-y\|>r\\ \|x-x'\|>r\\ \|x'-y\|>r}} \mathbf{1}_{W_{n,r}}(x)\,\mathbf{1}_{W_{n,r}}(x')\,v(x-x',r)\,u_m(x'-x,r)\,u_m(x-x',y-x',r)$$
$$f(y-x')\mathrm{d}x'\,\mathrm{d}y\,\mathrm{d}x.$$

Finally, substituting $z = x-x'$ and $w = y-x'$, and the fact that $u_m(-z,r) = u_m(z,r)$ results in equation (14).

4) If x, x' belong to the process of cluster members triggered by the same point of the cluster center process, we can write the first term of equation (19) as

$$\xi_{CMM}(r) \equiv \mathbb{E}\left[\sum_{y\in\Phi_c}\sum_{x,x'\in\Phi_m^{(y)}}^{\neq} \mathbf{1}_{W_{n,r}}(x)\,\mathbf{1}_{H(x,r)}(\Phi-\delta_x)\,\mathbf{1}_{W_{n,r}}(x')\,\mathbf{1}_{H(x',r)}(\Phi-\delta_{x'})\right]$$
$$= \lambda_c\int\mathbb{E}\Big[\sum_{x,x'\in\tilde{\Phi}_m^{(y)}}^{\neq} \mathbf{1}_{W_{n,r}}(x)\mathbf{1}_{H(x,r)}(\Phi+\tilde{\Phi}_m^{(y)}+\delta_y-\delta_x)\mathbf{1}_{W_{n,r}}(x')$$
$$\mathbf{1}_{H(x',r)}(\Phi+\tilde{\Phi}_m^{(y)}+\delta_y-\delta_{x'})\Big]\mathrm{d}y,$$

where the second equality is obtained by using the Slivnyak-Mecke Theorem for Φ. Then, conditioning on Φ and using the Slivnyak-Mecke Theorem for $\tilde{\Phi}_m^{(y)}$, results in

$$\xi_{CMM}(r) = \lambda_c\lambda_m^2 \iiint\limits_{\substack{\|x-y\|>r\\ \|x-x'\|>r\\ \|x'-y\|>r}} \mathbf{1}_{W_{n,r}}(x)\,\mathbf{1}_{W_{n,r}}(x')\,\mathbb{P}\left(\Phi\in H(x,x',r)\right)\mathbb{P}\left(\tilde{\Phi}_m^{(y)}\in H(x,x',r)\right)$$
$$f(y-x)\,f(y-x')\mathrm{d}x\,\mathrm{d}x'\,\mathrm{d}y$$

$$= \lambda_c\lambda_m^2 \iiint\limits_{\substack{\|x-y\|>r\\ \|x-x'\|>r\\ \|x'-y\|>r}} \mathbf{1}_{W_{n,r}}(x)\,\mathbf{1}_{W_{n,r}}(x')\,v(x-x',r)\,u_m(x-x',y-x',r)\,f(y-x)$$
$$f(y-x')\mathrm{d}x\,\mathrm{d}x'\,\mathrm{d}y.$$

Making the substitution $z = y - x$ and $w = y - x'$, and simplification results in equation (15).

5) When x, x' belong to cluster member processes triggered by different points of the cluster center process, the first term of equation (19) is

$$\xi_{CCMM}(r) \equiv \mathbb{E}\left[\sum_{y,y'\in\Phi_c}^{\neq}\sum_{x\in\Phi_m^{(y)}}\sum_{x'\in\Phi_m^{(y')}} \mathbf{1}_{W_{n,r}}(x)\,\mathbf{1}_{H(x,r)}(\Phi-\delta_x)\,\mathbf{1}_{W_{n,r}}(x')\,\mathbf{1}_{H(x',r)}(\Phi-\delta_{x'})\right]$$

$$= \lambda_c^2 \iint \mathbb{E}\Big[\sum_{x\in\tilde{\Phi}_m^{(y)}}\sum_{x'\in\tilde{\Phi}_m^{(y')}} \mathbf{1}_{W_{n,r}}(x)\,\mathbf{1}_{H(x,r)}(\Phi+\tilde{\Phi}_m^{(y)}+\tilde{\Phi}_m^{(y')}+\delta_y+\delta_{y'}-\delta_x)$$
$$\mathbf{1}_{W_{n,r}}(x')\,\mathbf{1}_{H(x',r)}(\Phi+\tilde{\Phi}_m^{(y)}+\tilde{\Phi}_m^{(y')}+\delta_y+\delta_{y'}-\delta_{x'})\Big]\,\mathrm{d}y\,\mathrm{d}y',$$

where (as before) the second equation is obtained by using the extended Slivnyak-Mecke Theorem for Φ. Conditioning on Φ, and then using the Slivnyak-Mecke Theorem sequentially for $\tilde{\Phi}_m^{(y)}$ and $\tilde{\Phi}_m^{(y')}$ results in

$$\xi_{CCMM}(r) = \lambda_c^2\lambda_m^2 \iiiint\limits_{\substack{\|x-x'\|>r\\ \|x-y\|>r\\ \|x-y'\|>r\\ \|x'-y\|>r\\ \|x'-y'\|>r\\ \|y-y'\|>r}} \mathbf{1}_{W_{n,r}}(x)\,\mathbf{1}_{W_{n,r}}(x')\,\mathbb{P}\left(\Phi\in H(x,x',r)\right)\,\mathbb{P}\left(\tilde{\Phi}_m^{(y)}\in H(x,x',r)\right)$$
$$\mathbb{P}\left(\tilde{\Phi}_m^{(y')}\in H(x',x,r)\right)\,f(x-y)\,f(x'-y')\,\mathrm{d}x\,\mathrm{d}x'\,\mathrm{d}y\,\mathrm{d}y'$$

$$= \lambda_c^2\lambda_m^2 \iiiint\limits_{\substack{\|x-x'\|>r\\ \|x-y\|>r\\ \|x-y'\|>r\\ \|x'-y\|>r\\ \|x'-y'\|>r\\ \|y-y'\|>r}} \mathbf{1}_{W_{n,r}}(x)\,\mathbf{1}_{W_{n,r}}(x')\,v(x-x',r)\,u_m(x-x',y-x',r)$$
$$u_m(x'-x,y'-x,r)\,f(x-y)\,f(x'-y')\,\mathrm{d}x\,\mathrm{d}x'\,\mathrm{d}y\,\mathrm{d}y'.$$

Finally, substituting $w = x - x'$, $z = x - y$, and $z' = x' - y'$, and the fact that $u_m(-w,-w-z',r)$ is equal to $u_m(w,-w-z'+w,r)$, which in turn is equal to $u_m(w,-z',r)$ results in equation (16).

Therefore, the first term of equation (19) in its entirety is given by

$$\mathbb{E}\left[\sum_{x,x'\in\Phi}^{\neq}\mathbf{1}_{W_{n,r}}(x)\mathbf{1}_{H(x,r)}(\Phi-\delta_x)\,\mathbf{1}_{W_{n,r}}(x')\,\mathbf{1}_{H(x',r)}(\Phi-\delta_{x'})\right] = \xi_{CC}(r) + 2\big(\xi_{CM}(r)+\xi_{CCM}(r)\big)+$$
$$\xi_{CMM}(r)+\xi_{CCMM}(r).$$

ACKNOWLEDGMENT

This work was supported by the European Commission in the framework of the FP7 Network of Excellence in Wireless COMmunications NEWCOM# (contract n.318306). Jesper Møller was supported by the Danish Council for Independent Research—Natural Sciences, grant 12-124675, "Mathematical and Statistical Analysis of Spatial Data", and by the Centre for Stochastic Geometry and Advanced Bioimaging, funded by a grant from the Villum Foundation.

REFERENCES

[1] J. G. Andrews, F. Baccelli, and R. K. Ganti, "A tractable approach to coverage and rate in cellular networks," *CoRR*, vol. abs/1009.0516, 2010.

[2] F. Baccelli and B. Blaszczyszyn, *Stochastic Geometry and Wireless Networks, Volume II - Applications*. NoW Publishers, 2009, vol. 4.

[3] ——, "Stochastic Geometry and Wireless Networks Volume 1: THEORY," *Foundations and Trends in Networking*, vol. 3, pp. 249–449, 2009.
[4] H. Dhillon, R. Ganti, F. Baccelli, and J. Andrews, "Modeling and analysis of k-tier downlink heterogeneous cellular networks," *Selected Areas in Communications, IEEE Journal on*, vol. 30, no. 3, pp. 550–560, 2012.
[5] L. Heinrich, "Asymptotic behaviour of an empirical nearest-neighbour distance function for stationary poisson cluster processes," *Mathematische Nachrichten*, vol. 136, no. 1, pp. 131–148, 1988.
[6] J. Mecke, "Stationäre zufällige Maße auf lokalkompakten Abelschen Gruppen," *Zeitschrift für Wahrscheinlichkeitstheorie und verwandte Gebiete*, vol. 9, pp. 36–58, 1967.
[7] N. Miyoshi and T. Shirai, "A cellular network model with Ginibre configurated base stations," 2012. [Online]. Available: http://www.is.titech.ac.jp/research/research-report/B/B-467.pdf
[8] J. Møller, *Lectures on Random Voronoi Tessellations*, ser. Lecture Notes in Statistics 87. Springer-Verlag, New York, 1994.
[9] ——, "Shot noise Cox processes," *Advances in Applied Probability*, vol. 35, pp. 4–26, 2003.
[10] J. Møller and G. L.Torrisi, "Generalised shot noise Cox processes," *Advances in Applied Probability*, pp. 48–74, 2005.
[11] J. Møller and R. P. Waagepetersen, *Statistical Inference and Simulation for Spatial Point Processes*. Chapman and Hall/CRC, Boca Raton, 2004.
[12] J. Neyman and E. Scott, "Statistical approach to problems of cosmology," *Journal of the Royal Statistical Society: Series B (Statistical Methodology)*, vol. 20, pp. 1–43, 1958.
[13] I. Riedel, R. Habendorf, E. Zimmermann, and G. Fettweis, "Multiuser transmission in cellular systems with different sector configurations." in *VTC Fall*. IEEE, 2008, pp. 1–5. [Online]. Available: http://dblp.uni-trier.de/db/conf/vtc/vtc2008f.html⇵RiedelHZF08
[14] V. Suryaprakash and G. Fettweis, "A stochastic examination of the interference in heterogeneous radio access networks," in *Wireless Optimization Conference (WiOpt), 2013 IEEE*, May 2013.
[15] G. L. Torrisi and E. Leonardi, "Large deviations of the interference in the Ginibre network model," *CoRR*, vol. abs/1304.2234, 2013.